

Texture edge smoothing and sharpening algorithm based on iterative non-local guided model

Ahmad Fauzan Kadmin^{1,2*}, Rostam Affendi Hamzah^{1,2}, Nasharuddin Zainal³, Shamsul Fakhar Abd Gani^{1,2} and Nabil Jazli⁴

Centre for Telecommunication Research and Innovation (CETRI), Universiti Teknikal Malaysia Melaka, Durian Tunggal, 76100 Melaka, Malaysia¹

Fakulti Teknologi Dan Kejuruteraan Elektronik Dan Komputer, Universiti Teknikal Malaysia Melaka, Durian Tunggal, 76100 Melaka, Malaysia²

Faculty of Engineering and Built Environment, Universiti Kebangsaan Malaysia, 43600 Bangi, Selangor, Malaysia³

IT Support Department, Amcorp Services Sdn Bhd, Petaling Jaya 46050 Selangor, Malaysia⁴

Received: 02-August-2024; Revised: 14-January-2025; Accepted: 22-January-2025

©2025 Ahmad Fauzan Kadmin et al. This is an open access article distributed under the Creative Commons Attribution (CC BY) License, which permits unrestricted use, distribution, and reproduction in any medium, provided the original work is properly cited.

Abstract

Image smoothing and sharpening are crucial operations in image processing, underpinning a wide array of applications across computer vision, medical imaging, and remote sensing. These processes are essential for delineating object details from noise, which is vital in fields such as graphics, computational photography, and computer vision. Despite their importance, achieving an ideal balance between smoothing and sharpening is challenging due to trade-offs and the presence of various types of noise and irregularities in real-life images. Traditional methods, such as Gaussian or median filtering (MF) for smoothing and Laplacian or unsharp masking for sharpening, often introduce artifacts or fail to preserve crucial details. This work proposes a cutting-edge image filter that used iterative non-local guided model (inLG), designed to be edge-aware and minimize halo artifacts. The primary objective is to enhance texture edge smoothing performance while preserving essential details and sharpening critical features in digital images. The filter's effectiveness is demonstrated through applications in image enhancement, evaluated through quantitative and qualitative, confirming its capability. The experimental results demonstrate the algorithm's superior performance, achieving a mean squared error (MSE) of 0.276, a peak signal-to-noise ratio (PSNR) of 59.82 dB, and a structural similarity index (SSIM) of 0.999. These results surpass traditional methods, offering a balanced trade-off between edge preservation and noise reduction.

Keywords

Image processing, Image smoothing, Image sharpening, Edge-aware filtering, Noise reduction, Detail enhancement.

1.Introduction

Image smoothing and sharpening are essential operations in image processing, serving a wide range of applications in domains like computer vision, medical imaging, and remote sensing [1]. Amidst the burgeoning applications spanning graphics, computational photography, and computer vision, the imperative of texture smoothing and sharpening emerges as a cornerstone, delineating the delineation between object details and noise [2, 3].

Image smoothing is performed to minimize noise and undesired details while maintaining significant structures and features, whereas image sharpening is intended to improve edges and intricate details for enhanced visual perception and analysis [4].

The challenge is to maintain the delicate balance between these two processes, since excessive smoothing may result in the loss of essential information, whereas over-sharpening could increase noise and artefacts [5]. Therefore, it is fundamental to build advanced techniques that integrate both smoothing and sharpening functionalities to properly manage this trade-off across various applications.

*Author for correspondence

However, fundamental tradeoffs and real-life image noise and defects make it challenging to balance texture smoothing and sharpening [6]. Traditional smoothing methods such as Gaussian or median filtering (MF) blur edges and textures, reducing visibility. Laplacian or unsharp masking may enhance noise however produce undesirable distortions, resulting in visually mediocre images that are unsuitable for analysis [7]. Recent advances in image processing have led to non-local window and iterative refinement-based filtering approaches to address these challenges. Non-local filtering methods use image redundancy to compare patches rather than pixels [8]. This method reduces noise and retains details better. The guided filter (GF) and its variations are popular for their computational efficiency and effectiveness in detail enhancement and denoising. Applying an input image or high-quality features, iterative guided filtering (iGF) improves the filtering process [9]. This improves smoothing and sharpening control and reduces artefacts. Numerous research has shown that non-local and iGF work in image-processing applications. Presented a non-local means filter (NLM) that outperforms existing magnetic resonance imaging (MRI) noise removal methods [10]. An iGF, as proposed by [11], employs a globally optimised technique known as the iterative self-guided image filter (isGIF), which is an extension of the GF assumptions. This method yields high-quality edge-preserving filtering outcomes by utilising the input image as the guidance image. Recently, adaptive gain techniques have been studied to tune sharpening effects to image dynamics. Smoothing and sharpening are often treated separately despite their relationship to one another.

The main aim of this work is to present the conceptualization and implementation of the proposed filter and evaluate its effectiveness with the most advanced techniques available. The objective of this paper also is to produce a technique that enhances the performance of texture edge smoothing while preserving essential details and sharpening important features in digital images. The main contributions of this work are the development of a novel edge-aware image filter that combines non-local windowing and iGF for texture smoothing and sharpening. The filter is designed to preserve object boundaries while minimising halo artifacts and offers a tunable parameter for seamless transitions between smoothing and sharpening modes. By addressing the limitations of existing methods, the quality of processed images was enhanced by the proposed

approach for various applications, including image enhancement, depth-of-field simulation, and image fusion. Comprehensive evaluations using subjective assessments and objective metrics demonstrate the filter's effectiveness and versatility in tackling contemporary challenges in image processing.

The rest of this paper's organization is as follows: Section 2 describes related works of guided, non-local and others related filters in achieving optimal accuracy, while Section 3 describes the proposed algorithm in detail. Section 4 and Section 5 describe the result and discussion, followed by a conclusion and future work in Section 6.

2. Literature review

This section focuses on the study that has been proposed with guided, non-local and others related filters in achieving optimal accuracy for texture smoothing and sharpening.

2.1 Image non-local filter

Non-local filters utilise image patch similarity rather than pixel-wise similarity. These filters utilise the inherent redundancy and self-similarity present in natural images to reduce noise and enhance fine details. The NLM technique, developed by [12], assigns weights to pixels based on the similarity of surrounding patches to perform non-local filtering. This method achieves impressive results in noise reduction by effectively preserving fine textures and structures, outperforming traditional local filters in handling complex noise patterns. However, it is associated with high computational complexity and is inefficient for highly textured images. In smoothing, non-local filter focusing on aspects such as selecting the size of patches, determining similarity measures, and improving computational efficiency. Non-local filters have been employed to enhance the clarity of images by enhancing edges and fine details while simultaneously lowering noise to provide sharpening effects while avoiding the occurrence of halos and ringing. Non-local filters are more effective than typical sharpening methods in situations with low signal-to-noise ratios. They are computationally intensive because they compare patches across a vast search window and have trouble distinguishing noise from textures in highly detailed or low-contrast regions. An ideal method aims to achieve comparable control over the local filter behaviour without the necessity of normalising to preserve the local brightness level by considering the complex impact on local brightness and contrast. An analytical model is obtained for the approximation filter with single

parameter proving that it can achieved desired quality and similarity for image smoothing, sharpening, and detail enhancement [13].

Proposed a method using non-local filter that uses a variable window size to implement computed tomography (CT) images enhancement and minimise noises which affected the CT abdomen structure yielding improved visualization of anatomical details, with advantages including adaptive noise reduction and enhanced structure preservation, but limitations such as increased computational complexity and potential difficulty in fine-tuning window sizes for varying noise levels [14]. A self-similarity NLM approach was also proposed by [15, 16] to improve improved curvelet that produced better peak signal-to-noise ratio (PSNR) value which performed better better than discrete wavelet transform with an NLM filter. Additionally, a two-phase ultrasound image de-speckling framework by [17] utilized NLM filtering for de-speckling and edge preservation on anisotropic diffused images, achieving a PSNR improvement of 2.06% to 46.68% over existing methods with advantages such as superior edge retention and effective speckle noise reduction, but with limitations including potential over-smoothing in highly textured regions and increased computational demands.

Muniraj and Dhandapani [18] described a method to enhance underwater images affected by suspended particles causing poor visibility and color distortions. This method includes a modified color correction, an adaptive look-up-table (LUT), and an edge-preserving filter. Improvements were made through color correction in the LAB color space, enhancement of the luminance (L) component using contrast-limited adaptive histogram equalization (CLAHE), sharpening, gamma correction, and further color correction of chrominance (A and B) components. Contrast enhancement was achieved via an adaptive LUT, followed by a fast local Laplacian filter (FLLF) for edge preservation and texture smoothing, and histogram normalization for color balancing. Non-local edge-aware filtering methods were enhanced by incorporating two complementary spatial trees, improving upon typical methods that use a minimum spanning tree (MST) [19]. This new approach demonstrated effectiveness in image denoising, JPEG artifact removal, tone mapping, detail enhancement, and colorization, but facing limitations in scalability to high-resolution images and potential inefficiency in handling highly complex textures.

2.2Image GF

GF utilise local linear models to dynamically integrate guidance and filtering images to obtain certain outcomes. The GF framework utilises a guidance image to guide the filtering process, enabling the preservation of edges and enhancement of details. The filter works by performing local linear transformations on both the guiding and filtering images, resulting in a filtered output that preserves the structural details of the guidance image [20]. Several studies have explored the application of GF for image smoothing, aiming to reduce noise and enhance image quality while preserving important details. In addition to smoothing, GF have been effectively utilized for image sharpening, allowing for the enhancement of edges and fine details while suppressing noise. Research in this area focuses on optimizing GF parameters to achieve desired sharpening effects while minimizing artifacts such as halos and edge distortions [21].

A fabric defect detection through improvements in GF and was proposed by [22] with a novel defect detection algorithm. The study found that using a Gaussian filter as the input image and the original image as the guidance image for the GF enhanced edge preservation and sharpening while maintaining detail, achieving a processing time of 26.2 ms per image. The detection algorithm, which incorporates the improved GF and illumination correction, demonstrated a defect detection rate of 97.35% and a processing time of 158.1 ms, meeting real-time requirements. It is offering advantages such as improved detection sensitivity and robustness to noise but facing limitations in handling highly textured fabrics and potential challenges with real-time processing. Another study by [23] explores image enhancement techniques focusing on improving contrast, restoration, noise reduction, and sharpening through multi-guided filtering (mGF). This method uses multiple guided images in joint filtering to retain structure information and employs a regularization term to ensure consistency among filtering outputs. Experimental results indicate that this approach significantly improves the PSNR, and overall image quality compared to traditional methods with advantages including better preservation of image details, enhanced contrast, and effective noise reduction. However, its limitations include increased computational cost due to the use of multiple guided images and potential challenges in handling images with highly complex or dynamic structures.

Further, advancements in thermal infrared image processing are discussed, emphasizing subpixel temperature retrieval and super-resolution enhancement. The proposed method combines high spatial resolution visible band images with thermal infrared images using multiresolution superpixel low-rank representation and residual correlation [24]. This approach enhances spatial characteristics, suppresses structural noise, and preserves spectral information, achieving a root-mean-square error of less than 1 K while significantly improving classification accuracy. Additionally, an improved weighted guided image filter (iWGIF) is introduced by [25] for enhancing synthetic-aperture radar images by simultaneously smoothing homogeneous regions and preserving heterogeneous regions. Finally, a novel fuzzy logic-based edge detection technique for X-ray images is presented, demonstrating significant improvements in edge quality and detection accuracy. Despite these advancements, challenges remain in optimizing GF techniques for specific applications, suggesting future research should explore deep learning-based approaches and scalability issues for high-resolution and real-time applications.

2.3 Image bilateral filter

This section discusses bilateral filtering (BF) as a powerful technique for image smoothing while preserving edges and fine details. Unlike traditional filters, BF consider both spatial proximity and intensity similarity between pixels, assigning weights based on these factors [26]. This approach effectively reduces noise in regions with similar intensities while maintaining sharp edges, making it superior for complex textures and noise reduction tasks. Recent studies emphasize optimizing parameters like spatial and intensity decay rates to achieve desired smoothing effects and enhance image quality without sacrificing detail.

A comprehensive evaluation of various filtering techniques was conducted, including the MF for smoothing, the Butterworth filter for sharpening, and the Inverse filter for restoration, using performance metrics such as PSNR and structural similarity index (SSIM) [27, 28]. The results demonstrate the efficacy of these filters in improving image and signal detection accuracy across different applications. Notably, adaptive filtering techniques like the least mean square (LMS) filter for electroencephalogram (EEG) signals and adaptive BF for image enhancement show promising results in noise reduction and feature preservation. The results show improved image quality and noise reduction,

advantages such as effective edge preservation and restoration, but limitations including potential blurring with the MF and the computational complexity of the Butterworth and Inverse filters for high-resolution images.

Furthermore, a novel adaptive BF method is proposed for infrared image enhancement, combining edge detection operators with BF to improve detail enhancement and noise suppression [29, 30]. This method integrates edge detection principles into the convolution kernel design, enhancing its capability to handle infrared image characteristics effectively, with results demonstrating improved detail preservation and noise reduction, advantages such as better edge clarity and reduced artifacts, but limitations including increased computational cost and potential challenges in fine-tuning parameters for different infrared image conditions.

In summary, the previous methods demonstrate the effectiveness of NLM, GF, and BF in enhancing image quality through noise reduction, detail preservation, and edge sharpening. NLM excel in handling complex noise but are computationally expensive. GFs, effective for defect detection and multi-image enhancement, face challenges in real-time processing and computational cost. BF offer strong edge preservation but struggle with parameter optimization for specific applications. Despite their successes, these methods encounter limitations in scalability, real-time processing, and handling complex textures.

3. Proposed algorithm

Numerous methods exist and the most popular is the averaging of value in image smoothing and sharpening in a local window based on the filter type aggregation. A widely popular approach is the use of the GF developed by [31], which utilizes local linear models to dynamically integrate guidance and filtering images. This method is often combined with the adaptive support weight (ASW) technique [32, 33]. ASW assigns adaptive weights to pixels within a support window based on spatial distance and intensity or color similarity, enabling effective noise reduction while preserving sharp edges. Although a well-developed method, there are still issues with reversal artifacts, generating halo artifacts at sharp edges and susceptible to the lack of texture. Hence, [34, 35] employed a slightly different technique using the BF for smoothing and sharpening that effectively reduces noise in regions with similar intensities while maintaining sharp edges, making it superior for

complex textures and noise reduction tasks. The techniques of smoothing and sharpening are essential for enhancing image quality and extracting valuable information. These techniques are often applied through various filters, each addressing specific issues related to image texture as shown *Figure 1*. Noise in images can arise from various sources such as sensor inaccuracies, environmental conditions, or transmission errors, leading to graininess and random variations in pixel intensity. Smoothing filters, such as Gaussian blur, MF, and average filter, are designed to mitigate these issues by averaging pixel values in a local neighborhood. This process helps in reducing the high-frequency components associated with noise while preserving the low-frequency components related to the actual content of the image. However, excessive smoothing can lead to a loss of important details and blurring of edges, which are crucial for identifying objects and textures in an image.

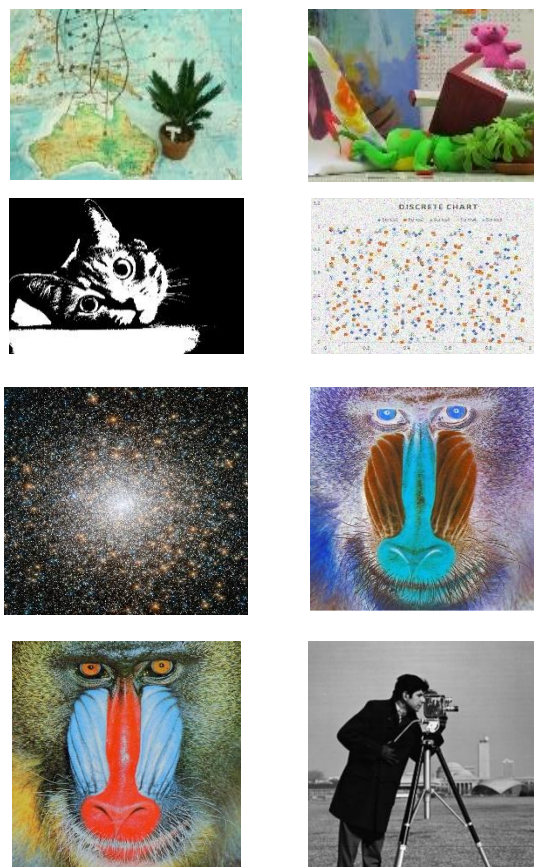


Figure 1 Image texture with different scenarios

On the other hand, this iterative non-local guided model (inLG) is used to enhance the edges and fine details of an image as shown in *Figure 2*, making the texture appear more defined and crisper. The inLG

was selected for its unique ability to simultaneously enhance edges and preserve fine details while minimizing common issues like halo artifacts and texture loss. Unlike traditional edge-preserving filters, this method leverages non-local similarity and iterative refinement, making it particularly effective for handling complex textures and low-contrast regions where conventional methods struggle. The use of an iterative process ensures progressive enhancement of image details and adaptive smoothing, surpassing the limitations of one-shot methods. A refined non-local cost function introduced that balances noise suppression and detail retention more effectively than existing non-local approaches. By coupling NLM with GF, the method optimally combines structural guidance with patch-based similarity, addressing texture loss and edge enhancement simultaneously. The method's ability to differentiate between noise and texture in intricate or subtle image regions is a key improvement over prior technique.

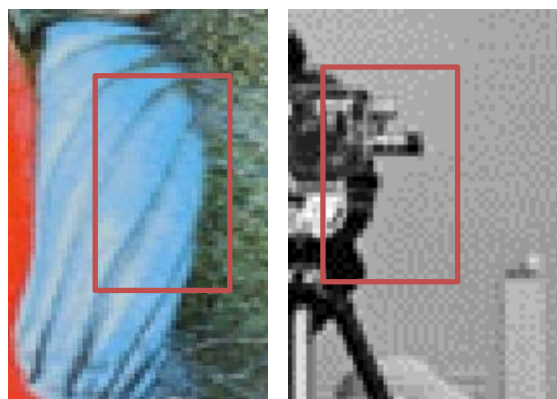


Figure 2 Edge texture for smoothing and sharpening

This is achieved by emphasizing the high-frequency components, which correspond to abrupt changes in intensity values. Sharpening filters, such as the Laplacian filter, unsharp mask, and high-pass filter, highlight these variations, thus enhancing edges and fine details. This technique is particularly useful in applications where precise texture and edge detection are critical, such as medical imaging, remote sensing, and industrial inspection. However, over-sharpening can introduce artifacts and amplify noise, leading to a distorted representation of the original image. Balancing smoothing and sharpening in image processing is a delicate task that requires careful consideration of the specific application and the nature of the image data. Advanced techniques often employ a combination of both, utilizing algorithms that adaptively apply smoothing and sharpening

based on the local characteristics of the image. This approach ensures that noise is effectively reduced without compromising the clarity and detail necessary for accurate image analysis. The filter in this work is using the NLM of pixel values from the input image based on neighbouring pixels as the guided imaging. The overall process for this work is shown as in Figure 3. Figure 3 provides a step-by-step visual representation of the proposed inLG for texture edge smoothing and sharpening. It outlines the workflow of the algorithm, emphasizing the integration of NLM and iGF for enhanced image processing.

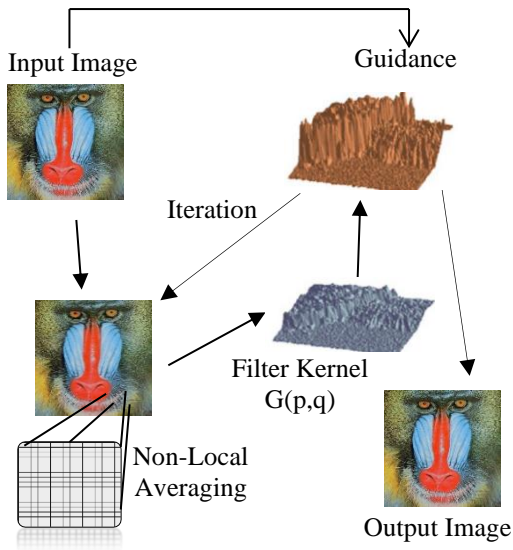


Figure 3 Smoothing and sharpening algorithm based on inLG

The original image is fed into the algorithm as the starting point. This image typically contains noise, low contrast, or texture irregularities that need correction. Then, the algorithm calculates the NLM values for each pixel based on the similarity of surrounding patches. This step leverages redundancy and self-similarity in the image to reduce noise while preserving essential details. The pixel cost is selected in this work as the guidance throughout the filtering process. Initially, the filtering starts with determining the non-local value averaging of the pixel employed by [36] expressed in Equation 1 as follows to achieve effective noise reduction while retaining fine textures and structures:

$$NL(p)_n = \frac{1}{c(p)} \int_{\Omega} I_n(p) f(p, q) dq \quad (1)$$

where Ω denotes the area of the non-local cost and $NL(p)_n$ represents the filtered value at point p while n_{NL} states the number of iterations. $I(p)$ is the pixel value at point p , q and $C(p)$ refers to the normalising factor. These components ensure proper normalization, preserving the brightness and contrast levels of the denoised image. $F(p, q)$ indicates the weighting function to determine how closely related the average cost at the point p is to the average cost at the point q . The $f(p, q)$ of the non-local weighting function is given by Equation 2 as follows:

$$f(p, q) = e^{-\frac{|D(q)_{q \in w_q} - D(p)_{p \in w_p}|^2}{(sd)^2}} \quad (2)$$

where $D(q)$ and $D(p)$ are the local mean value of the average cost surrounding q and p under support window w_q and w_p to capture the intensity similarity, allowing the filter to adapt to the local structure and avoid blending dissimilar regions, while sd refers to the filtering parameter of standard deviation by adjusting sd , the trade-off between noise reduction and detail preservation can be controlled. Then, the non-local weighting function $G_{p,q}(NL_n)$ determines the contribution of neighboring pixels q to the processing of the center pixel p . It ensures that pixels with higher similarity have a greater influence on the output. The NLM values through the filter kernel of $G_{p,q}(NL_n)$ as applied by [31] and expressed by Equation 3 as follows:

$$G_{p,q}(NL_n) = \frac{1}{|w|^2} \sum_{q \in w_g} \left(1 + \frac{(NL(p)_{n-1} - \mu_{g,n-1})(NL(q)_{n-1} - \mu_{g,n-1})}{\sigma_{g,n-1}^2 + \epsilon} \right) \quad (3)$$

where NL_n refers to the NLM cost at n -th iteration and p represents the coordinates pixel of interest (x, y). The size of support window, $r \times r$ is denoted as w_g and w represents the number of pixels in the support window, w_g . The weighting term incorporates both local and non-local information, balancing between preserving texture and smoothing noise. The $NL(p)$ and $NL(q)$ are the value from the NLM with q and p representing the neighbouring pixel in the support window and the center pixel. The control element for the smoothness term is represented by the letter ϵ . The μ_g and σ_g indicate the guidance cost mean and variance of cost values allow the method to adapt to local intensity variations which are given by Equations 4 and 5 as follows:

$$\mu_g = \frac{1}{|w|} \sum_{q \in w_g} NL(q), \quad (4)$$

$$\sigma_g = \frac{1}{|w|} \sum_{q \in w_g} NL(q) - \mu_g, \quad (5)$$

The final cost value from the guidance at this process is expressed as in Equation 6 as follows:

$$iGF_n(p) = G_{p,q}(NL_n)I_n(p) \quad (6)$$

where the $G_{p,q}(NL_n)$ is the weight of output filter kernel and $I(p)$ refers to the pixel value at point p computation at n -th iteration from input image. The non-local weighting ensures that edge and texture information is preserved, while the input intensity reflects the original image details. Iterative refinement through n iterations ensures that the filter balances noise reduction, detail retention, and computational stability. It is pivotal in applications like denoising, sharpening, and texture enhancement. The model iteratively refines the filtering process by updating the weights and reapplying the non-local GF. Each iteration progressively improves noise suppression and detail preservation. After several iterations, the processed image is generated, featuring enhanced edges, reduced noise, and clearer textures.

The USC-SIPI Image Database is the standard online benchmarking datasets used in this work [37]. The USC-SIPI Image Database is a collection of digitized images contributed from The University of South Carolina (USC) under Signal and Image Processing Institute and maintained primarily to support research in image processing, image analysis, and machine vision. This work using standard images from the Miscellaneous volume consisting of 44 images, 16 color and 28 monochromes with sizes 14 images 256x256, 26 images 512x512, and 4 images 1024x1024. This standard online benchmarking data sets have several images that are needed to establish the accuracy of this algorithm. Furthermore, it is also to establish the efficacy of other researchers' methods. Therefore, this is ideal for conducting comparison for the texture edge of smoothing and sharpening in this work. The selection of test images in image processing research and algorithm development is a critical step that significantly impacts the evaluation and performance of the techniques being tested. In many instances, test images are selected to represent natural or typical scenes that a particular class of processing techniques would encounter in real-world applications. These images are usually representative of common scenarios such as landscapes, portraits, urban scenes, and other everyday visuals. The rationale behind using these types of images is to ensure that the developed algorithms can effectively handle the kind of data they are likely to process in practical applications. Many images in the USC-SIPI database are of high resolution, enabling detailed analysis of

fine textures and edges. This makes it ideal for evaluating algorithms designed to enhance details and preserve subtle image features. The database includes images with varying levels of noise, providing a suitable platform for testing denoising capabilities while preserving essential textures and edges. The database includes images that mimic real-world scenarios, such as complex textures, varying lighting conditions, and diverse edge structures. This ensures the algorithm's applicability in practical, real-world situations. By working with these representative images, researchers can better gauge the practical utility and robustness of their algorithms. This approach helps in validating the generalizability of the techniques, ensuring they perform well across a wide range of typical use cases. Figure 4 shows step by step the process of texture edge smoothing and sharpening algorithm based on inLG.

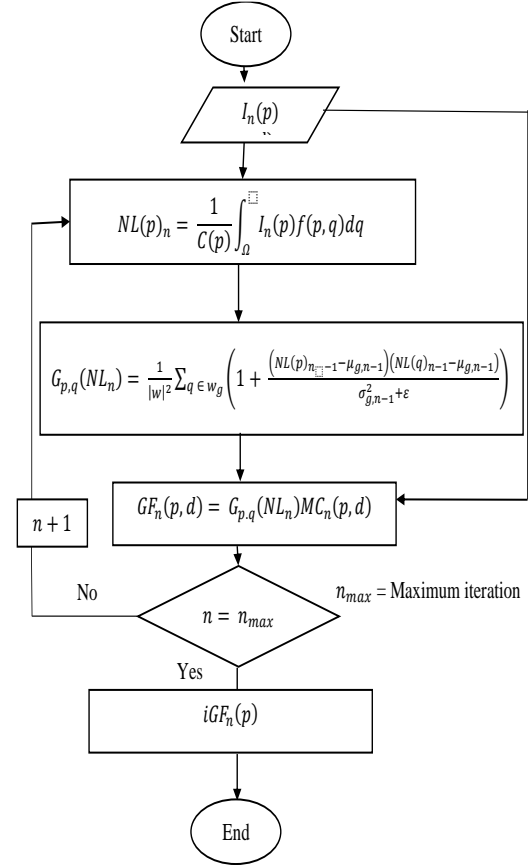


Figure 4 inLG algorithm flow

Building upon the strengths and addressing the limitations of existing methods such as GF and BF, the inLG was developed to overcome challenges like halo artifacts and texture loss often observed in


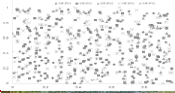





traditional approaches. While GF excels at edge preservation and BF effectively balances spatial proximity and intensity similarity, both methods encounter issues when handling complex textures or low-contrast regions. The proposed inLG model integrates the patch-based similarity of NLM with the structural guidance of iGF. This novel combination allows for more robust edge enhancement and detail sharpening, offering a tunable framework that adapts to various image characteristics.

4.Result

4.1Dataset and experimental setup

An experimental setup was developed to aid in the development and testing of this filter using several images from the USC-SIPI database focused on Cat_JPEG, Chart_Grayscale, Mandrill, Mandrill_Inverted, Mandrill_Grayscale, Nebula_Reference and Nebula_Zoomed which consist of different types of scenarios, environment and texture as shown in *Table 1*.

Table 1 Tested images with different scenarios and textures

No.	Name	Image	Features
1	Cat_JPEG.jpg		Black and white with thin line texture
2	Chart_Grayscale.bmp		Grayscale with random thin and dot textures
3	Mandrill.bmp		RGB with many thin line's textures and edges
4	Mandrill_Inverted.bmp		Inverted RGB with many thin line's textures and edges
5	Mandrill_Grayscale.bmp		Grayscale with many thin line's textures and edges
6	Nebula_Reference.jpg		RGB with random small texture and edges and impulse noise
7	Nebula_Zoomed.bmp		RGB with random small texture and edges and impulse noise and halo artefacts

These images were not modified in any manner and did not contain any type of image enhancement to be used for the purpose of providing a quantitative and qualitative evaluation of filter application. Several images were employed, as stated earlier, to demonstrate the adaptability of the proposed algorithm. The results from these images were compared and discussed with several established methods accordingly. All the experiments were executed using the Python programming language,

OpenCV library and the hardware of a personal computer with the central processing unit (CPU) Intel Xeon E5-2650, 2.6GHz and 64G RAM.

In this study, multiple analyses were conducted, encompassing both quantitative and qualitative evaluations. The quantitative assessment focused on the accuracy performance of each image, utilizing three standard image assessment metrics: mean squared error (MSE), PSNR, and SSIM. MSE

measures the average of the squared differences between corresponding pixels in the input and processed images, PSNR compares the fidelity of the processed images, and SSIM evaluates the similarity to human visual perception by considering changes in image structure and local patterns. For the qualitative evaluation, the processed images were analyzed based on visual perception and texture quality. The final output of this model, the filtered image, was also compared with those obtained using other standard image filtering approaches. This study does not prioritize runtime or computational efficiency because its primary focus is on demonstrating the qualitative and quantitative superiority of the inLG algorithm for texture edge smoothing and sharpening. The reported performance metrics, such as MSE, PSNR, and SSIM, highlight the method's effectiveness in enhancing image quality, which is the primary research objective. Moreover, runtime and computational efficiency are highly hardware dependent. Significant improvements can be achieved through hardware upgrades, such as leveraging graphics processing unit (GPU) for parallel processing or utilizing optimized libraries for matrix operations. GPU acceleration can dramatically reduce the runtime of the inLG algorithm by parallelizing computations for patch similarity, weighting functions, and iterative updates.

4.2 Comparison of quantitative performance

In this work, there were two types of evaluations performed: quantitative and qualitative evaluation. The algorithm for the model is assigned as inLG as a

reference when comparing with other established methods. The first step in gaining the optimal parameters for the equations in this research was to determine the variables and parameters that were used in the equations. Since these parameters reflected the final accuracy of the inLG, it was essential to identify the parameters that were able to produce the best outcomes. However, in many instances these parameters took different values.

All the constant parameters were originally planned to a minimum value and were gradually increased until the average error output attained a minimum value. Consequently, this method contributed to the efficient maximise usage of the selected parameters. The selection of the parameters began with window size computation and continued one at a time followed with sigma value and number of iterations as shown in *Figure 5* and *Figure 6* which are reflected in the MSE and PSNR result. The first parameter selected was the window size for the inLG. There was a minimum value of 0.4291 of MSE and a maximum of PSNR value at 51.80 dB when the algorithm ran with window size of 3. According to the graph of *Figure 5* and 6, when window size was increased uniformly in sequence, the MSE increased sharply then gradually decreased in uniform sequence, while the differences between each size steadily increased. While when the window size increased, the PSNR value started to decrease steadily until it remained constant after window size of 9.

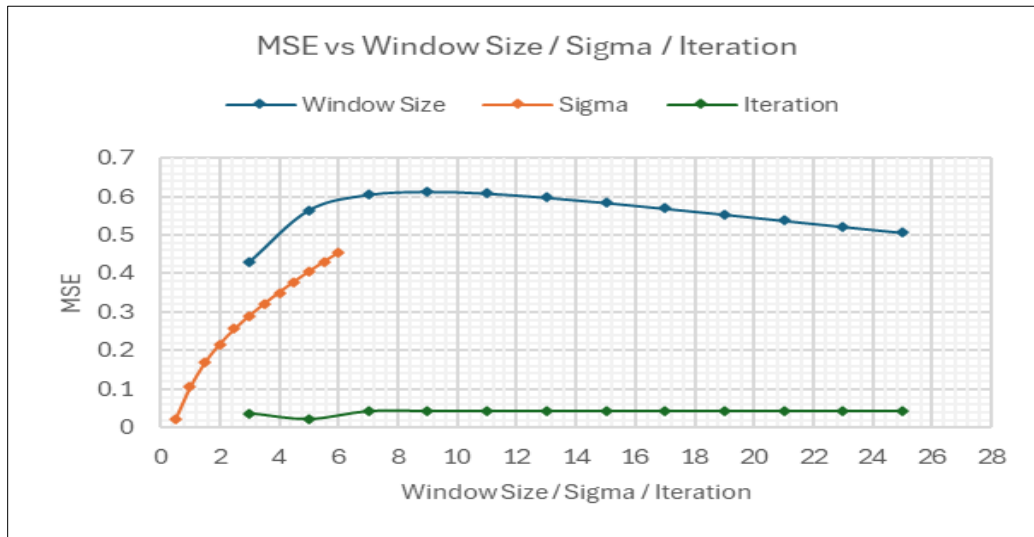


Figure 5 Parameter tuning for window size, sigma and iteration with MSE result

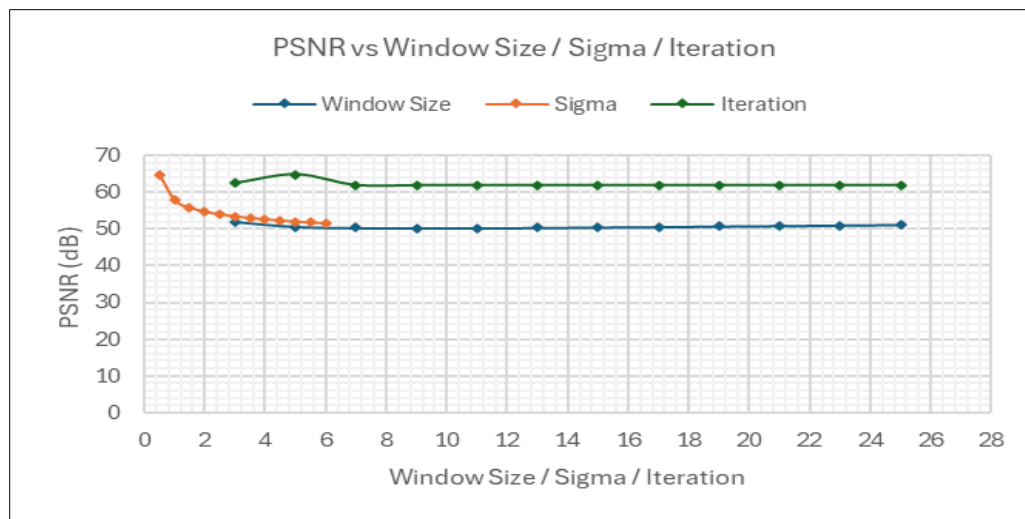


Figure 6 Parameter tuning for window size, sigma and iteration with PSNR result

The second parameter determined in this algorithm was the sigma value. Based on the graph, the MSE and PSNR increased and reduced dramatically when the value of sigma increased in sequence and the minimum value window size remained constant at 3. The lowest value of MSE is at 0.021 while the maximum value of PSNR is at 64.82 dB when the sigma value = 0.5. The third parameter used was the number of iterations which indicated the lowest value of 0.021 for MSE and the maximum PSNR at the value of 64.82 dB. This occurred when the number of iterations was settled at 5 iterations. Based on the graph, the MSE increased slightly while the PSNR reduced slightly after 9 iterations and remained constant after that. The final values from these parameters tuning were employed as evaluations for the MSE, PSNR, SSIM and visual parameters. However, as more optimal settings were continuously applied to the parameters of the proposed algorithm, the images became clearer and sharper, improving the images quality and accuracy. *Table 2* provides an overview of the parameters used and respective values in this work.

Table 2 Summary of parameters used in this work

S. No.	Image	Value
1	Window Size	3×3
2	Sigma Value	0.5
3	Number of Iterations	0.942

As stated earlier, seven prominent benchmarking images were employed to determine the algorithm's adaptability. The performance of this algorithm validated using both quantitative and qualitative evaluation. The results from these images were

compared and discussed with several established methods accordingly. *Table 3* presents the qualitative performance based on MSE, whereas *Table 4* provides the PSNR. *Tables 5* exhibits quantitative performance based on SSIM. The established methods comparison consists of BF, NLM, GF and iGF to further evaluate the accuracy of the algorithm. The proposed inLG algorithm performed well when compared to the other methods used according to the evaluation tables of MSE, PSNR and SSIM as shown in *Table 3*, *Table 4* and *Table 5*. *Table 3* presents a comparison of MSE values for different image processing methods. MSE measures the average squared difference between the original and processed images, with lower MSE values indicating better quality (less distortion). The proposed inLG produced the lowest average at 0.276 of MSE value from 7 images. The inLG also produced the lowest value of MSE for 5 images compared with other methods. The closest accuracy for MSE was the GF which has the second lowest MSE value at 0.381. The highest of MSE which with the almost error is iGF at 4.987. The inLG consistently demonstrates the lowest MSE values across the images, indicating superior performance in preserving image quality with minimal distortion.

Table 4 compares the PSNR values, measured in decibels (dB), for various image processing methods. PSNR is a widely used metric to assess the quality of a processed image compared to its reference image. Higher PSNR values generally indicate better quality, with less distortion introduced by the processing method. The inLG also performed well in PSNR evaluation which contributed the highest average

value of PSNR at 59.82 dB. The closest PSNR value is contributed by GF method at 54.15 with 10.5% difference compared with the inLG. It is observed that the inGL PSNRs performed poorly for Mandrill, Mandrill_Grayscale and Mandrill_Inverted images when compared with the BF and GF. GF shows the highest PSNR, followed by inLG and BF for Mandrill image. NLM and iGF exhibit significantly lower values, indicating poorer performance. For Mandrill_Grayscale, BF has the highest PSNR, with inLG also performing well. NLM and iGF show

much lower values. While for Mandrill_Inverted image, similar to the original Mandrill image, GF performs best, followed by inLG and BF, while NLM and iGF have lower PSNR values. These images consist of a lot of fine small textures and boundaries that contributed to many noises. However, the inLG PSNR values for these images are still better than other methods such as NLM and iGF. The inLG consistently demonstrates the highest PSNR values across the images, indicating its strong capability in preserving image quality.

Table 3 MSE comparison based on methods

No	Image	BF	NLM	GF	iGF	inLG
1	Cat_JPEG	0.140	0.491	0.022	0.228	0.012
2	Chart_Grayscale	0.226	0.227	0.186	0.615	0.091
3	Mandrill	0.942	9.341	0.601	7.681	0.686
4	Mandrill_Grayscale	0.128	5.286	0.709	8.712	0.435
5	Mandrill_Inverted	0.942	9.343	0.601	7.681	0.686
6	Nebula_Reference	0.988	6.306	0.139	3.845	0.001
7	Nebula_Zoomed	1.387	0.524	0.405	6.147	0.024
Average		0.679	4.501	0.381	4.987	0.276

Table 4 PSNR comparison based on methods (dB)

No	Image	BF	NLM	GF	iGF	inLG
1	Cat_JPEG	56.65	51.21	64.64	54.54	67.11
2	Chart_Grayscale	54.57	54.55	55.41	50.23	58.53
3	Mandrill	48.38	38.42	50.33	39.27	49.76
4	Mandrill_Grayscale	57.04	40.89	49.62	38.72	51.74
5	Mandrill_Inverted	48.38	38.42	50.33	39.27	49.76
6	Nebula_Reference	48.18	40.13	56.67	42.28	77.85
7	Nebula_Zoomed	46.70	50.93	52.04	40.24	64.18
Average		51.42	44.94	54.15	43.51	59.82

Table 5 presents a comparison of SSIM values across different image processing methods. SSIM is a metric used to measure the similarity between two images. The closer the SSIM value is to 1, the more similar the processed image is to the reference image. Table 5 provides valuable insights into the effectiveness of

various image processing methods, with BF and inLG standing out as particularly reliable techniques for preserving image quality. The inLG and BF always establish high SSIM values across all images, indicating their robustness and effectiveness in maintaining structural similarity.

Table 5 SSIM comparison based on methods

No	Image	BF	NLM	GF	iGF	inLG
1	Cat_JPEG	0.998	0.996	0.999	0.998	0.999
2	Chart_Grayscale	0.999	0.999	0.999	0.999	0.999
3	Mandrill	0.999	0.989	0.999	0.992	0.999
4	Mandrill_Grayscale	0.999	0.970	0.997	0.960	0.998
5	Mandrill_Inverted	0.999	0.989	0.999	0.992	0.999
6	Nebula_Reference	0.999	0.988	0.999	0.993	1.000
7	Nebula_Zoomed	0.998	0.998	0.999	0.991	0.999
Average		0.999	0.954	0.990	0.989	0.999

4.3 Comparison of qualitative performance


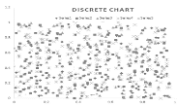



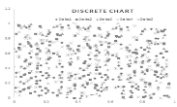



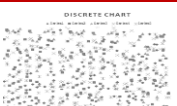



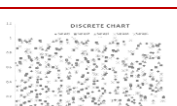










Table 6 compares various image filter methods by displaying different images for four categories of photos: Cat, Chart, Mandrill, and Nebula. Difference images serve to emphasise the disparities between the

original and processed images, offering a visual tool to evaluate the effectiveness of each method. Smaller intensity visuals in the difference images suggest a lower number of differences, which implies superior performance. Based on the Cat image, the BF shows

a low-intensity difference indicating moderate performance while NLM is likely to show higher intensity difference, reflecting poorer performance compared to other methods. The GF has very low-intensity difference, indicating excellent performance and iGF perform better than NLM but not as well as GF. The proposed work inLG has the lowest intensity difference, showing superior performance compared with other methods. While for the Chart image, inLG shows the lowest intensity difference, indicating best performance followed by the GF with low-intensity differences. The NLM is comparable to BF but likely to show higher intensity differences while the iGF shows higher differences, indicating poorer

performance. The Mandrill and Nebula images provide complexity in textures which show the inLG outperformed other methods with lowest intensity differences. The iGF produced the highest intensity differences that contributed the poorest performance. The inLG and GF demonstrated the best performance, with the lowest intensity differences in the difference images, indicating minimal discrepancies from the original. The BF shows moderate performance, with more discrepancies than inLG and GF. The NLM and iGF show higher intensity differences, indicating lower performance in preserving the original image quality.

Table 6 Comparison of methods based on difference images

Method	Cat	Chart	Mandrill	Nebula
Original				
BF				
NLM				
GF				
iGF				
<i>inLG</i>				

The performance of the algorithm was further evaluated with qualitative evaluation through visual inspection of the textures and boundaries of the images. *Table 7* and *8* show the comparison of methods using visual inspection based on texture and smoothing. The areas shown by the red box in *Table 6* are the regions that contributed to the complex textures and boundaries consisting of noises such as speckles and gaussian noise. The colours in these regions had much high contrast with each other, such as the difference between brighter blue and darker

blue with the same blue spectrum but distinctive intensities.

Based on this result, it shows that the BF a sharp textures and edges at the boundaries but the speckle and gaussian noise still remains which affects the quality of this image. The performance of the NLM is almost similar to the BF which have sharp texture and edges along with intensity increased. However, there are patches of speckle and gaussian noises in the region. The GF produced a clearer and sharper texture and edges if compared with the iGF which

produced blurry boundaries indicating over smoothing. Both methods show less speckle and gaussian noises in the region. The inLG algorithm removes the speckle and gaussian noises in the regions especially for the Mandrill image, the textures and edges at the boundaries are clearer and sharper while preserving the intensity.

Table 8 shows the comparison of methods with the enlarge regions of textures and textureless at the boundaries. Two types of images of used which are

the Mandrill_Inverted and Mandrill_Grayscale to analyse the performance in colour and grayscale structures. To establish the algorithm in larger low-texture regions was significantly more difficult and complex due to the similarity of the pixel intensities. The textureless or low texture regions were always regarded as having inadequate texture information, and the colours in these regions had much less contrast with each other. The original image shows noises at plain textures and the boundaries consist of uneven textures.

Table 7 Comparison of methods for texture and smoothing






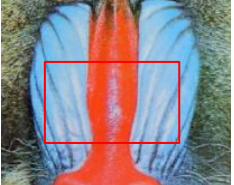

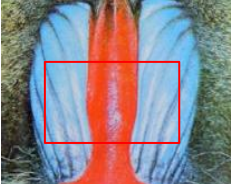

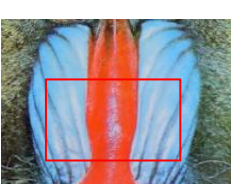





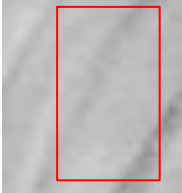

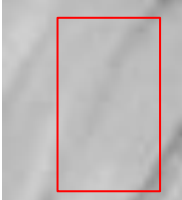





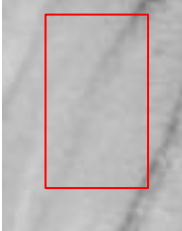
Method	Nebula_Reference	Mandrill
Original		
BF		
NLM		
GF		
iGF		
<i>inLG</i>		

Table 8 Comparison of textures and boundaries based on methods

Method	Mandrill Inverted	Mandrill Grayscale
Original		
BF		
NLM		
GF		
iGF		
<i>inLG</i>		

Observations from the analyzed images indicate that the proposed algorithm, *inLG*, effectively produces smooth results in plain, textureless areas by removing noise and generating sharp edges around boundaries, with fewer unwanted pixels compared to other methods. Moreover, the BF and NLM experienced edge distortion, which was apparent at the boundaries, and the GF and iGF produced blurred edges. The BF, GF and *inLG* preserved textured

details although these algorithms successfully removed the noises. The proposed algorithm generates clear, sharp and detailed contour of textures, compared with the iGF which produced over-smoothing textures. The proposed algorithm performed effectively well in regions with complex textures, which resulted in better sharpening and smoothing of images.

5. Discussion

5.1 Observations and implications

The observations from the proposed inLG reveal its robust performance in balancing texture edge smoothing and sharpening. The algorithm demonstrated superior results in reducing noise, preserving edges, and enhancing fine details compared to traditional methods like BF, NLM, GF, and iGF. Quantitative metrics such as MSE, PSNR, and SSIM validated its efficacy, with the inLG consistently achieving the lowest MSE, highest PSNR, and near-optimal SSIM values across diverse image scenarios. One notable anomaly observed in the results is the underperformance of the inLG algorithm for the Mandrill images compared to its exceptional performance with the Nebula images. The Mandrill images are characterized by complex textures with thin lines and intricate patterns, which challenge the algorithm's ability to differentiate between fine details and noise. This complexity likely causes a slight trade-off between smoothing and detail preservation, leading to higher MSE and lower PSNR values for these images. Conversely, the Nebula images feature broader, less intricate textures with smoother transitions between colors and intensities. The inLG algorithm handles such structures more effectively, achieving higher PSNR and SSIM values due to its strong edge preservation and noise reduction capabilities.

The performance of the inLG is highly sensitive to parameter choices, with optimal values such as a 3x3 window size, $\sigma = 0.5$, and five iterations achieving the best balance between noise reduction, edge preservation, and computational efficiency. Smaller window sizes and lower σ values preserve fine details but may inadequately suppress noise, while larger windows and higher σ values enhance smoothing at the expense of texture clarity. Iterative refinement improves quality up to a point, after which diminishing returns or artifacts may occur. These parameters introduce trade-offs between accuracy and computational cost, emphasizing the importance of fine-tuning or adaptive parameter selection to suit specific image characteristics.

The visual inspection further supports these findings, as the inLG effectively handled complex textures and boundaries while maintaining smoothness in low-texture regions. This capability is crucial for applications in medical imaging, remote sensing, and industrial inspection, where preserving critical details is essential. The iterative nature of the algorithm allows progressive enhancement, making the texture

appear more defined and crisper without introducing artifacts like halos or excessive smoothing. In comparison with other established methods, the inLG showed significant improvements. The BF, while effective in preserving edges, struggled with texture loss and noise suppression in complex regions. NLM provided good noise reduction but suffered from high computational costs and reduced effectiveness in low-contrast areas. GF performed well in edge preservation but introduced halo artifacts and lacked the capability to handle intricate textures. iGF exhibited over-smoothing in certain scenarios. The inLG, however, addressed these limitations by integrating non-local averaging and GF iteratively, ensuring better texture retention and artifact-free outputs.

5.2 Study limitations

Despite its strengths, the inLG has some limitations. The iterative nature of the algorithm increases computational complexity, making it less suitable for real-time applications. Additionally, the selection of parameters such as σ and window size require careful tuning to achieve optimal results, which could be challenging for non-expert users. While the algorithm handles complex textures effectively, its performance may degrade with extremely noisy or heavily degraded images. Future work should address these limitations by incorporating adaptive parameter selection and exploring optimization techniques, such as parallel processing or GPU acceleration, to enhance computational efficiency. These observations underscore the potential of the inLG as a versatile and effective tool in image processing, particularly for applications requiring precise edge and texture management. A complete list of abbreviations is listed in *Appendix I*.

6. Conclusion and future work

In this work, we have proposed a novel texture edge smoothing and sharpening algorithm that combines the strengths of GF and NLM within an inLG. The primary aim was to enhance the performance of texture edge smoothing while preserving essential details and sharpening important features in digital images. Through a series of experiments, the proposed algorithm demonstrated superior performance in balancing edge preservation and noise reduction compared to traditional methods. The GF's ability to perform edge-preserving smoothing, combined with the NLM effectiveness in reducing noise by averaging similar patches, resulted in a robust algorithm that outperforms existing approaches. The iterative nature of the model further

refined the results by progressively enhancing the image quality with each iteration. Quantitative and qualitative assessments confirmed the efficacy of the proposed method, showcasing improved visual quality, higher MSE and PSNR, with acceptable SSIM scores with value of MSE at 0.276, PSNR at 59.82 dB and SSIM at 0.999 that outperforms traditional methods.

While the current algorithm uses fixed parameters for inLG, future work could explore adaptive parameter selection techniques that dynamically adjust based on local image characteristics to further enhance performance. The iterative nature of the algorithm, while beneficial for quality, increases computational complexity. Research into optimization techniques, such as parallel processing or GPU acceleration, could make the algorithm more practical for real-time applications. Extending the algorithm to video sequences can be investigated, ensuring temporal consistency while applying texture edge smoothing and sharpening. This would be particularly useful in video enhancement and restoration tasks. Combining the proposed method with deep learning frameworks could yield further improvements. For instance, incorporating a deep neural network to learn optimal filter parameters or using the proposed method as a pre-processing step for deep learning models in computer vision tasks. The inLG presents a significant advancement in texture edge smoothing and sharpening. With further research and development, this approach has the potential to be widely adopted in various image processing applications.

Acknowledgment

The authors express their sincere gratitude to the Ministry of Higher Education (MoHE) Malaysia and Universiti Teknikal Malaysia Melaka (UTeM) for providing the necessary funding to complete this study through the Translational Research Grants Programme (Grant No. JPT.S (BPKI) 2000/016/018/017 Jld 10 (7)).

Conflicts of interest

The authors have no conflicts of interest to declare.

Data availability

The data used in this study was obtained from the University of South Carolina (USC) through the Signal and Image Processing Institute Database (USC-SIP). This dataset is publicly accessible.

Author's contribution statement

Ahmad Fauzan Kadmin: Conceptualization, investigation, data collection, writing – review and editing. **Nabil:** Writing – review and editing. **Rostam Affendi**

Hamzah: Supervision, writing – review and editing. **Nasharuddin Zainal:** Data collection, examine and correct the manuscript, supervision. **Shamsul Fakhur Abd Gani and Nabil Jazli:** Conceptualization, investigation, examine and correct the manuscript.

References

- [1] Woodhouse C. The astrophotography manual image processing fundamentals. Routledge; 2024.
- [2] Zhao Y, Jia W, Chen Y, Wang R. Fast blind decontouring network. *IEEE Transactions on Circuits and Systems for Video Technology*. 2022; 33(2):478-90.
- [3] Wang F, Chen F, Tang J, Huang M. Generic skeleton object detection framework with gradient maps. In *proceedings of the 15th international conference on digital image processing 2023* (pp. 1-8). ACM.
- [4] Demir Y, Kaplan NH. Low-light image enhancement based on sharpening-smoothing image filter. *Digital Signal Processing*. 2023; 138:104054.
- [5] Farahani SS, Reshadinezhad MR, Fatemeh SE. New design for error-resilient approximate multipliers used in image processing in CNTFET technology. *The Journal of Supercomputing*. 2024; 80(3):3694-712.
- [6] Weli MM, Abdullah OM. Hybrid smoothing and sharpening filters using the spatial domain: literature review. *International Research Journal of Innovations in Engineering and Technology*. 2024; 8(2):51-60.
- [7] Li J. A review of fingerprint image enhancement based on Gabor filter. In *international conference on image, vision and intelligent systems 2022* (pp. 519-25). Singapore: Springer Nature Singapore.
- [8] Wang H. Application of non-local mean image denoising algorithm based on machine learning technology in visual communication design. *Journal of Intelligent & Fuzzy Systems*. 2023; 45(6):10213-25.
- [9] Qiao Z, Wen X, Zhou X, Qin F, Liu S, Gao B, et al. Adaptive iterative guided filtering for suppressing background noise in ptychographical imaging. *Optics and Lasers in Engineering*. 2023; 160:107233.
- [10] Sun Z, Angelis G, Meikle S, Calamante F. MRI tractography-guided PET image reconstruction regularisation using connectome-based nonlocal means filtering. *Physics in Medicine & Biology*. 2023; 68(13):1-14.
- [11] He L, Xie Y, Xie S, Jiang Z, Chen Z. Iterative self-guided image filtering. *IEEE Transactions on Circuits and Systems for Video Technology*. 2024; 34(8):7537-49.
- [12] Liu X, Wu Z, Wang X. The validity analysis of the non-local mean filter and a derived novel denoising method. *Virtual Reality & Intelligent Hardware*. 2023; 5(4):338-50.
- [13] Rekha H, Samundiswary P. Image denoising using fast non-local means filter and multi-thresholding with harmony search algorithm for WSN. *International Journal of Advanced Intelligence Paradigms*. 2023; 24(1-2):92-109.
- [14] Seo KH, Kang SH, Shim J, Lee Y. Optimization of smoothing factor for fast non-local means algorithm in

- high pitch based low-dose computed tomography images with tin-filter. *Radiation Physics and Chemistry*. 2023; 206:110762.
- [15] Sun Z, Meikle S, Calamante F. CONN-NLM: a novel CONNectome-based non-local means filter for PET-MRI denoising. *Frontiers in Neuroscience*. 2022; 16:1-14.
- [16] Yang K, Chen C, Hu X, Yu H. Denoising algorithm based on multi-feature non-local mean filtering for Monte Carlo rendered images. *Journal of System Simulation*. 2022; 34(6):1259-66.
- [17] Thakur N, Khan NU, Sharma SD. A two phase ultrasound image de-speckling framework by nonlocal means on anisotropic diffused image data. *Informatica*. 2023; 47(2):221-33.
- [18] Muniraj M, Dhandapani V. Underwater image enhancement by modified color correction and adaptive look-up-table with edge-preserving filter. *Signal Processing: Image Communication*. 2023; 113:116939.
- [19] Bu P, Wang H, Yang T, Zhao H. Linear time manageable edge-aware filtering on complementary tree structures. *Computers & Graphics*. 2024; 118:133-45.
- [20] Zhang X, Zhao W, Zhang W, Peng J, Fan J. Guided filter network for semantic image segmentation. *IEEE Transactions on Image Processing*. 2022; 31:2695-709.
- [21] Mishiba K. Fast guided median filter. *IEEE Transactions on Image Processing*. 2023; 32:737-49.
- [22] Teng M, Dali Y, Lingyan H. Fabric defect detection based on improved guided filter. *Wool Textile Journal*. 2017; 45(11):70-3.
- [23] Zuo Y, Xie J, Wang H, Fang Y, Liu D, Wen W. Gradient-guided single image super-resolution based on joint trilateral feature filtering. *IEEE Transactions on Circuits and Systems for Video Technology*. 2022; 33(2):505-20.
- [24] Xinyuan MI, Zhang Y, Zhang J. Spatial fusion enhancement of thermal infrared images based on multi-resolution analysis and low-rank guided filter. *National Remote Sensing Bulletin*. 2021; 25(11):2255-69.
- [25] Li Z, Zheng J, Senthilnath J. Simultaneous smoothing and sharpening using IWGIF. In *international conference on image processing 2022* (pp. 861-5). IEEE.
- [26] Yang Y, Xiong Y, Cao Y, Zeng L, Zhao Y, Zhan Y. Fast bilateral filter with spatial subsampling. *Multimedia Systems*. 2023; 29(1):435-46.
- [27] Gonzales AL, Ramos AL, Lacson JM, Go KS, Furigay RB. Optimizing image and signal processing through the application of various filtering techniques: a comparative study. In *novel & intelligent digital systems conferences 2023* (pp. 151-70). Cham: Springer Nature Switzerland.
- [28] Shehin AU, Sankar D. Adaptive bilateral filtering detection using frequency residuals for digital image forensics. In *29th international conference on systems, signals and image processing 2022* (pp. 1-6). IEEE.
- [29] Khetkeeree S, Thanakitivirul P. Hybrid filtering for image sharpening and smoothing simultaneously. In *35th international technical conference on circuits/systems, computers and communications 2020* (pp. 367-71). IEEE.
- [30] Lv H, Shan P, Shi H, Zhao L. An adaptive bilateral filtering method based on improved convolution kernel used for infrared image enhancement. *Signal, Image and Video Processing*. 2022; 16(8):2231-7.
- [31] He K, Sun J, Tang X. Guided image filtering. *IEEE Transactions on Pattern Analysis and Machine Intelligence*. 2012; 35(6):1397-409.
- [32] Liu H, Wang R, Xia Y, Zhang X. Improved cost computation and adaptive shape guided filter for local stereo matching of low texture stereo images. *Applied Sciences*. 2020; 10(5):1-17.
- [33] Toet A. Alternating guided image filtering. *Peer J Computer Science*. 2016; 2: 1-18.
- [34] Yang WJ, Tsai ZS, Chung PC, Cheng YT. An adaptive cost aggregation method based on bilateral filter and canny edge detector with segmented area for stereo matching. In *international workshop on advanced image technology 2019* (pp. 288-93). SPIE.
- [35] Hamzah RA, Ibrahim H, Hassan AH. Stereo matching algorithm based on per pixel difference adjustment, iterative guided filter and graph segmentation. *Journal of Visual Communication and Image Representation*. 2017; 42:145-60.
- [36] Wang G, Liu Y, Xiong W, Li Y. An improved non-local means filter for color image denoising. *Optik*. 2018; 173:157-73.
- [37] Webber AG. The USC-SIPI image database: version 6. USC-SIPI Report. 2018; 432: 1-24.



Ahmad Fauzan Kadmin is a Chartered Engineer and Professional Technologist, currently serving as a Senior Lecturer at Universiti Teknikal Malaysia Melaka (UTeM). He has over 16 years of experience in electronic and computer engineering, computer vision, and medical electronics. He holds a Bachelor's degree in Electronics Engineering from Universiti Sains Malaysia, a Master's degree in Computer & Communication Engineering from Universiti Kebangsaan Malaysia, and a Ph.D. in Computer Vision from Universiti Teknikal Malaysia Melaka.
Email: fauzan@utem.edu.my



Rostam Affendi Hamzah earned his Bachelor of Engineering in Electronic Engineering from Universiti Teknologi Malaysia. He obtained his Master of Science in Electronic System Design Engineering from Universiti Sains Malaysia in 2010 and his Ph.D. in Electronic Imaging from the same university in 2017. He is currently a Senior Lecturer at Universiti Teknikal Malaysia Melaka, where he teaches digital electronics, digital image processing, and embedded

systems. His research interests include Computer Vision, Pattern Recognition, and Digital Image Processing.
Email: frostamaffendi@utem.edu.my



Nasharuddin Zainal is an esteemed academic and prominent researcher in the field of Computer Engineering. He holds a Doctor of Engineering (Dr.Eng.) degree in International Development from the Tokyo Institute of Technology. Additionally, he has completed his Master of Engineering (M.Eng.) in Communication and Computer from Universiti Kebangsaan Malaysia, and a Bachelor of Engineering (B.Eng.) in Information Engineering (Computer Engineering) from Tokyo Institute of Technology. His research interests span a wide range of cutting-edge domains, including Image and Video Processing, Pattern Recognition, and Robotics.
Email: nasharuddin.zainal@ukm.edu.my



Shamsul Fakhar Abd Gani earned his Bachelor of Engineering (Computer Engineering) with Honours from Universiti Malaysia Perlis and his Master of Technology in Internet & Web Computing from the Royal Melbourne Institute of Technology, Australia. He is currently a Senior Lecturer at Universiti Teknikal Malaysia Melaka, where he primarily conducts research in computer vision.
Email: shamsulfakhar@utem.edu.my



Nabil Jazli completed his Bachelor of Engineering Technology Computer (Computer Systems) with honors from Universiti Teknikal Malaysia and is now pursuing his Master of Science in Electronic Engineering at Universiti Teknikal Malaysia Melaka. Currently, he is an IT Executive at Amcorp Group Berhad in the Information & Technology Division.
Email: nabil.jazli@amcorp.com.my

Appendix I

S. No.	Abbreviation	Description
1	ASW	Adaptive Support Weight
2	BF	Bilateral Filtering
3	CLAHE	Contrast-Limited Adaptive Histogram Equalization
4	CPU	Central Processing Unit
5	CT	Computed Tomography
6	EEG	Electroencephalogram
7	FLLF	Fast Local Laplacian Filter
8	GF	Guided Filter
9	GPU	Graphics Processing Unit
10	iGF	Iterative Guided Filtering
11	inLG	Iterative Non-Local Guided Model
12	isGIF	Iterative Self-Guided Image Filter
13	iWGIF	Improved Weighted Guided Image Filter
14		
15	LMS	Least Mean Square
16	LUT	Look-Up-Table
17	MF	Median Filtering
18	mGF	Multi-Guided Filter
19	MRI	Magnetic Resonance Imaging
20	MSE	Mean Squared Error
21	NLM	Non-Local Means Filter
22	MST	Minimum Spanning Tree
23	PSNR	Peak Signal-to-Noise Ratio
24	SSIM	Structural Similarity Index